Mon. Not. R. Astron. Soc. **399,** 1650–1662 (2009) doi:10.1111/j.1365-2966.2009.15404.x

Relic H II regions and radiative feedback at high redshifts

Andrei Mesinger,[1]★† Greg L. Bryan[2] and Zoltán Haiman[2]

[1]*Department of Astrophysical Sciences, Princeton University, Princeton, NJ 08544, USA*
[2]*Department of Astronomy, Columbia University, 550 West 120th Street, New York, NY 10027, USA*

Accepted 2009 July 14. Received 2009 July 10; in original form 2008 December 16

ABSTRACT

Ultraviolet (UV) radiation from early astrophysical sources could have a large impact on subsequent star formation in nearby protogalaxies, and in general on the progress of cosmological reionization. Theoretical arguments based on the absence of metals in the early Universe suggest that the first stars were likely massive, bright, yet short-lived, with lifetimes of a few million years. Here we study the radiative feedback arising from such stars using hydrodynamical simulations with transient UV backgrounds (UVBs) and persistent Lyman–Werner backgrounds (LWBs) of varying intensity. We extend our prior work in Mesinger et al., by studying a more typical region whose protogalaxies form at lower redshifts, $z \sim 13$–20, in the epoch likely preceding the bulk of reionization. We confirm our previous results that feedback in the relic H II regions resulting from such transient radiation is itself transient. Feedback effects dwindle away after ∼30 per cent of the Hubble time, and the same critical specific intensity of $J_{\rm UV} \sim 0.1 \times 10^{-21}$ erg s^{-1} cm^{-2} Hz^{-1} sr^{-1} separates positive and negative feedback regimes. This suggests that overall feedback is fairly insensitive to the large-scale environment, overdensity and redshift-dependent halo parameters, and can accurately be modelled in this regime with just the intensity of the impinging UVB. Additionally, we discover a second episode of eventual positive feedback in haloes which have not yet collapsed when their progenitor regions were exposed to the transient UVB. When exposed to the transient UVB, this gas suffers relatively little density depletion but a significant enhancement of the molecular hydrogen abundance, thus resulting in net positive feedback. This eventual positive feedback appears in all runs, regardless of the strength of the UVB. However, this feedback regime is very sensitive to the presence of Lyman–Werner radiation, and notable effects disappear under fairly modest background intensities of $J_{\rm LW} \gtrsim 10^{-3} \times 10^{-21}$ erg s^{-1} cm^{-2} Hz^{-1} sr^{-1}, assuming the region is optically thin for LW photons. Nevertheless, when exposed to the same LWB, haloes inside relic H II regions always have a higher H_2 abundance and shorter cooling times than haloes outside relic H II regions, allowing gas to cool faster once it finally begins to collapse on to the halo. We conclude that UV radiative feedback in relic H II regions, although a complicated process, seems unlikely to have a major impact on the progress of cosmological reionization, provided that present estimates of the lifetime and luminosity of a Population III star are accurate. More likely is that the build-up of the LWB ultimately governs the feedback strength until a persistent UV background can be established.

Key words: galaxies: high-redshift – cosmology: theory – early Universe.

1 INTRODUCTION

Semi-analytic models and numerical simulations predict that the first astrophysical objects formed at redshifts $z \gtrsim 20$. They form out of metal-free gas with inefficient fragmentation, thus numerical simulations predict that these first objects could be very massive ($M_* \gtrsim 100\,{\rm M}_\odot$), so-called Population III (Pop III) stars (Abel, Bryan & Norman 2002; Bromm, Coppi & Larson 2002; Yoshida, Omukai & Hernquist 2008). These stars would be short-lived, with lifetimes of ∼3 Myr, but could produce 10 times more ionizing photons per baryon than regular Population II stars (Schaerer 2002, 2003). Also, such star formation could have been somewhat

★Hubble Fellow.
†E-mail: mesinger@astro.princeton.edu

synchronized, given that these early objects formed in highly biased and clustered environments. Hence, Pop III stars could have a significant impact on subsequent generations of objects.

Indeed Pop III stars can strongly affect the progress of cosmological reionization (Cen 2003a,b; Haiman & Holder 2003; Wyithe & Loeb 2003), although their contribution is virtually unknown from first principles and is generally applied to simulations with a 'tuning knob' approach. Thus, ionizing photons from the first stars and lack thereof have been used to explain both early (e.g. Cen 2003b) and fairly late (e.g. Haiman & Bryan 2006) reionization, depending on which scenario was favoured when the works were published. Therefore, it is quite important to gain physical insight into how the radiation of the first stars impacted their surroundings.

Radiative feedback can be either positive or negative, in that it can enhance or suppress subsequent star formation. Positive feedback can result when the enhanced free-electron fraction from ionizing photons (e.g. Oh & Haiman 2002) or hydrodynamical shocks (Shapiro & Kang 1987) catalyzes the formation of molecular hydrogen (H_2). If the ionizing background 'turns off' (resulting in so-called relic H II regions), H_2 cooling can provide the dominant cooling channel at high densities and low temperatures. Conversely, negative feedback can result from heating by ionizing radiation which can photoevaporate gas in low-mass haloes (Efstathiou 1992; Barkana & Loeb 1999; Gnedin 2000; Dijkstra et al. 2004; Shapiro, Iliev & Raga 2004; Mesinger & Dijkstra 2008). Also, an active background of Lyman–Werner (LW) radiation (with photon energies in the 11.18–13.6 eV range) can dissociate H_2, thus decreasing the gas's cooling capabilities (e.g. Haiman, Rees & Loeb 1997; Ciardi, Ferrara & Abel 2000; Haiman, Abel & Rees 2000; Machacek, Bryan & Abel 2001; Wise & Abel 2007; O'Shea & Norman 2008).

Indeed, simulations find radiative feedback to be nuanced at very high redshifts. Positive feedback dominates in flash-ionized gas (O'Shea et al. 2005) or gas exposed to a weak transient ultraviolet background (UVB; Mesinger, Bryan & Haiman 2006, hereafter MBH06) such as might be present close to the edges of H II regions (Ricotti, Gnedin & Shull 2002; Kuhlen & Madau 2005). On the other hand, negative feedback in relic H II regions can occur in regions closer to the Pop III star (MBH06; Susa & Umemura 2006; Ahn & Shapiro 2007; Yoshida et al. 2007). Furthermore, radiative transfer effects can also impact the strength and sign of feedback (e.g. Iliev, Shapiro & Raga 2005; Susa & Umemura 2006; Abel, Wise & Bryan 2007; Whalen et al. 2008; Wise & Abel 2008b). Because of variations in the halo mass, collapse redshift, central baryon density, stellar spectrum and distance to the ionizing source, it is difficult to accurately deal with the large parameter space governing photoevaporation.

In MBH06, we attempted to tackle this issue with a statistical approach. By giving up on simulating 'realistic' (as much as this is possible given present uncertainties) relic H II regions left behind by deceased Pop III stars, we were able to explore larger swaths of parameter space and have a fairly large sample of second-generation objects. We did this by applying various uniform ultraviolet (UV) and LW backgrounds (LWBs) to our entire simulation box, and statistically comparing the resulting evolution against the fiducial run without radiation. Although this approach clearly does not realistically treat the photoionization around a particular source, it might provide a good statistical description of an ensemble of reionization studies. Clearly, at the onset of reionization not all haloes lie within H II regions, as they do in our models. Our primary purpose is not to simulate early reionization or the photoevaporation of well-formed Pop III haloes in detail (which would require radiative transfer) but to evaluate the impact of relic H II regions on the formation of haloes at later times. Our uniformly illuminated boxes provide an ensemble of evaporated haloes at high redshift that statistically sample the effects of early photoionization on the assembly of haloes and formation of cold dense gas at lower redshifts.

However, since our analysis in MBH06 focused on a highly biased region which went non-linear at a high redshift, we could not follow the evolution to redshifts much lower than $z \sim 20$. This meant that we could only extrapolate the observed trends suggesting that the feedback was transient. Oh & Haiman (2003) claim that, even in the presence of a weak LWB, excess entropy will eventually suppress star formation in protogalaxies forming inside relic H II regions. In MBH06, we were unable to conclusively verify or refute this claim.

In this work, we extend the study by MBH06 by analysing radiative feedback in a less-biased region, whose typical protogalaxies form at lower redshifts, $z \sim 13$–20. Given that the 5 yr *Wilkinson Microwave Anisotropy Probe* (*WMAP*) polarization data place a constraint on the reionization redshift (assuming instantaneous reionization) of $z = 11.0 \pm 1.4$ (Dunkley et al. 2009), such cosmological regions are likely to host the majority of feedback effects from Pop III stars, before a persistent UVB and/or a strong LWB become entrenched (e.g. Haiman, Rees & Loeb 1996). We apply the same statistical approach as in MBH06 and study various combinations of transient UVBs and persistent LWBs. As such, we attempt to provide a framework for analytically incorporating such radiative feedback into semi-analytic, and large-scale numerical and seminumerical studies.

In Section 2, we enumerate and describe the simulations which are used in this work. In Section 3, we study the initial radiative feedback caused by a transient UVB, adding a persistent LWB in Section 3.1. Then in Section 4, we describe a related mechanism that results in eventual positive feedback, regardless of the strength of the UVB. In Section 5, we discuss the impact of neglecting self-shielding. Finally, we offer our conclusions in Section 6.

Throughout this paper, we adopt the background cosmological parameters (Ω_Λ, Ω_M, Ω_b, n, σ_8, H_0) = (0.7, 0.3, 0.047, 1, 0.92, 70 km s^{-1} Mpc^{-1}), consistent with the measurements of the power spectrum of cosmic microwave background (CMB) temperature anisotropies by the first year of data from the *WMAP* satellite (Spergel et al. 2003). Although the 5 yr data prefer a slightly lower value of $\sigma_8 = 0.82$ (Dunkley et al. 2009; Komatsu et al. 2009) which somewhat delays structure formation, we keep the cosmology the same as in MBH06, to facilitate direct comparison. Unless stated otherwise, we quote all quantities in comoving units.

2 SIMULATIONS

We use the Eulerian adaptive mesh refinement (AMR) code ENZO, which is described in greater detail elsewhere (Bryan 1999; Norman & Bryan 1999). Our simulation volume is 1 $(h^{-1}\,\mathrm{Mpc})^3$, initialized at $z_\mathrm{init} = 99$ with density perturbations drawn from the Eisenstein & Hu (1999) power spectrum. Our root grid is 128^3. We have two additional static levels of refinement inside a central $0.25\,h^{-1}$ Mpc cube. In addition, grid cells inside the central region are allowed to dynamically refine so that the Jeans length is resolved by at least four grid zones and no grid cell contains more than four times the initial gas mass element. Each additional grid level refines the mesh length of the parent grid cell by a factor of 2. We allow for a maximum of 10 levels of refinement inside the refined central region, granting us a spatial resolution of $7.63\,h^{-1}$ pc. This comoving resolution translates to $0.36\,h^{-1}$ proper pc at $z = 20$.

Table 1. Summary of simulation runs.

Run name	$J_{21}^{\rm UV}$	$z_{\rm UVB,on}$	$z_{\rm UVB,off}$	$J_{21}^{\rm LW}$
Runs without an LWB				
NoUVB	0	NA	NA	0
Flash	–	25	25	0
Heat0.08	0.08	25	24.62	0
Heat0.8	0.8	25	24.62	0
Runs with an LWB				
LW10^{-4}_NoUVB	0	NA	NA	10^{-4}
LW10^{-4}_Heat0.8	0.8	25	24.62	10^{-4}
LW10^{-3}_NoUVB	0	NA	NA	10^{-3}
LW10^{-3}_Heat0.8	0.8	25	24.62	10^{-3}
LW10^{-2}_NoUVB	0	NA	NA	0.01
LW10^{-2}_Heat0.8	0.8	25	24.62	0.01
LW0.1_NoUVB	0	NA	NA	0.1
LW0.1_Heat0.8	0.8	25	24.62	0.1

As stated above, our simulation runs were set up to facilitate comparison with MBH06. Users interested in details of the simulations are encouraged to consult MBH06 and Machacek et al. (2001). There is one notable difference between our runs here and those in MBH06: our central refined region for these runs is *not* centred on the highest density region of the box. Instead, it is chosen to be more typical of the regions expected to host the bulk of haloes which form prior to any significant cosmological reionization. Specifically, the density inside our central $(0.25\,h^{-1}\,{\rm Mpc})^3$ corresponds to a 0.75σ mass fluctuation of an equivalent spherical volume (in MBH06, we studied a 2.4σ region). The less overdense region allows us to extend the analysis of MBH06 to lower redshifts and test the robustness of the conclusions of MBH06 on a less-biased and more typical region.

As shown in Table 1, we have performed four different runs without an LWB, distinguished by the duration or amplitude of the assumed UVB, and eight additional runs that include an additional constant LWB. Again, these runs are runs analogous to those in MBH06. For the UV radiation we assume an isotropic background flux with a $T = 2 \times 10^4$ K blackbody spectral shape, normalized at the hydrogen ionization frequency, $h\,\nu_{\rm H} = 13.6$ eV. This spectrum is softer than the $\sim 8 \times 10^4$ K blackbody spectrum predicted to be produced by Pop III stars (e.g. Schaerer 2002), which leads us to find a lower reionization temperature (by about a factor of 2) than we would have found with a harder spectrum. This results in outflow velocities (and therefore halo evacuation times) which are also too low by this factor.

The values of $J_{21}^{\rm UV}$ are shown in Table 1 in units of 10^{-21} erg s^{-1} cm^{-2} Hz^{-1} sr^{-1}. The NoUVB run contains no UV radiation, and serves mainly as a reference run. The Heat0.08 and Heat0.8 runs include a UVB with $J_{21}^{\rm UV} = 0.08$, 0.8, respectively. The value of $J_{21}^{\rm UV} = 0.08$ was chosen to correspond to the mean UV flux expected inside a typical H II region surrounding a primordial star (e.g. Alvarez, Bromm & Shapiro 2006). As we do not include dynamically expanding H II regions in our code, the Heat0.8 and Flash (in which the UVB is turned on for a negligibly short duration) runs can be viewed as extremes, corresponding to conditions close to the centre and close to the edge of the H II region, respectively. More generally, studying a range of values of $J_{\rm UV}$ is useful, since the radiative properties of high-redshift sources are uncertain. In the latter two runs, the UVB is turned on at $z_{\rm UVB,on} = 25$ and turned off at $z_{\rm UVB,off} = 24.64$. This redshift range corresponds to a typical theoretical stellar lifetime, $\sim$3 Myr, of an $\sim 100\,{\rm M}_\odot$ primordial (Pop-III) star (Schaerer 2002). The flash ionization run, Flash, instantaneously sets the gas temperature to $T = 15\,000$ K and the hydrogen neutral fraction to $x_{\rm H\,I} = 10^{-3}$ throughout the simulation volume, but involves no heating thereafter. Again, our adopted temperature is probably too low by a factor of 2 compared to gas heated by Pop III stars. Finally, the eight runs in the bottom half of the table repeat pairs of the NoUVB and Heat0.8 runs with four different constant LWBs ($J_{21}^{\rm LW} = 10^{-4}$, 0.001, 0.01 and 0.1, normalized at 12.87 eV in units of 10^{-21} erg s^{-1} cm^{-2} Hz^{-1} sr^{-1}, and assumed to be frequency independent within the narrow LW band).

We obtain the dark matter (DM) and baryonic mass of haloes, in the same manner as MBH06. Similarly, we use the fraction of total gas within the virial radius which is cold and dense (CD), $f_{\rm cd}$, as a proxy for the gas reservoir available to form stars. By cold, we mean gas whose temperature is $< 0.5T_{\rm vir}$, where $T_{\rm vir}$ is the halo's virial temperature (for how virial temperatures are associated with haloes in the simulation, see Machacek et al. 2001). By dense, we mean gas whose density is $> 10^{19}\ {\rm M}_\odot\,{\rm Mpc}^{-3} \approx 330\,{\rm cm}^{-3}$, roughly corresponding to the density at which the baryons become important to the gravitational potential in the core, taken to be an immediate precursor to primordial star formation (Abel et al. 2002).

Additionally, we discount haloes which have been substantially contaminated by the large (low-resolution) DM particles originally outside of our refined region which enter it as it becomes nonlinear. Specifically, we remove from our analysis haloes with an average DM particle mass greater than $\sim$140 per cent of the refined region's DM mass resolution, $747\,{\rm M}_\odot$. However, since there are small stochastic variations in the amount of contamination between the runs, we first apply this cut-off in the NoUVB run and then remove the same haloes from the analysis of the other runs. This way, we study the same haloes in each run.

Another possible source of contamination arises from closely separated haloes. If some CD gas belonging to a halo is within another halo's virial radius (most likely in the process of merging), the other halo could undeservedly be flagged as containing CD gas as well. To counteract this, we set $f_{\rm cd} = 0$ for all haloes without CD gas in their innermost spherical shell. CD gas invariably first forms close to the halo's core, where the cooling times are the shortest; thus haloes which contain CD gas at large radii but none in their core are most likely in the process of merging with a halo with genuine CD gas. Note that this algorithm is different than the one used in MBH06, where we discriminated based on mass and separation between haloes. In this work, such contamination was more prevalent and so we devised what proved to be a more robust means of discrimination.

Finally, we note that we do not include HD cooling in these simulations. As is shown in McGreer & Bryan (2008) and Yoshida et al. (2007), HD cooling is important in primordial haloes only in the density range 10^2–10^6 cm^{-3}, where H_2 can bring the temperature below about 200 K. Therefore it does not change the amount of CD gas, our primary diagnostic (although it would lead to relatively small changes in the predicted masses of the resulting stars).

3 TRANSIENT FEEDBACK FOLLOWING A TRANSIENT ULTRAVIOLET BACKGROUND

We first wish to confirm whether our conclusions in MBH06 also apply to this new sample of haloes, which form at later times in a less overdense region of the universe. In MBH06, we found the following. The UVB ionizes and heats the gas in our simulation

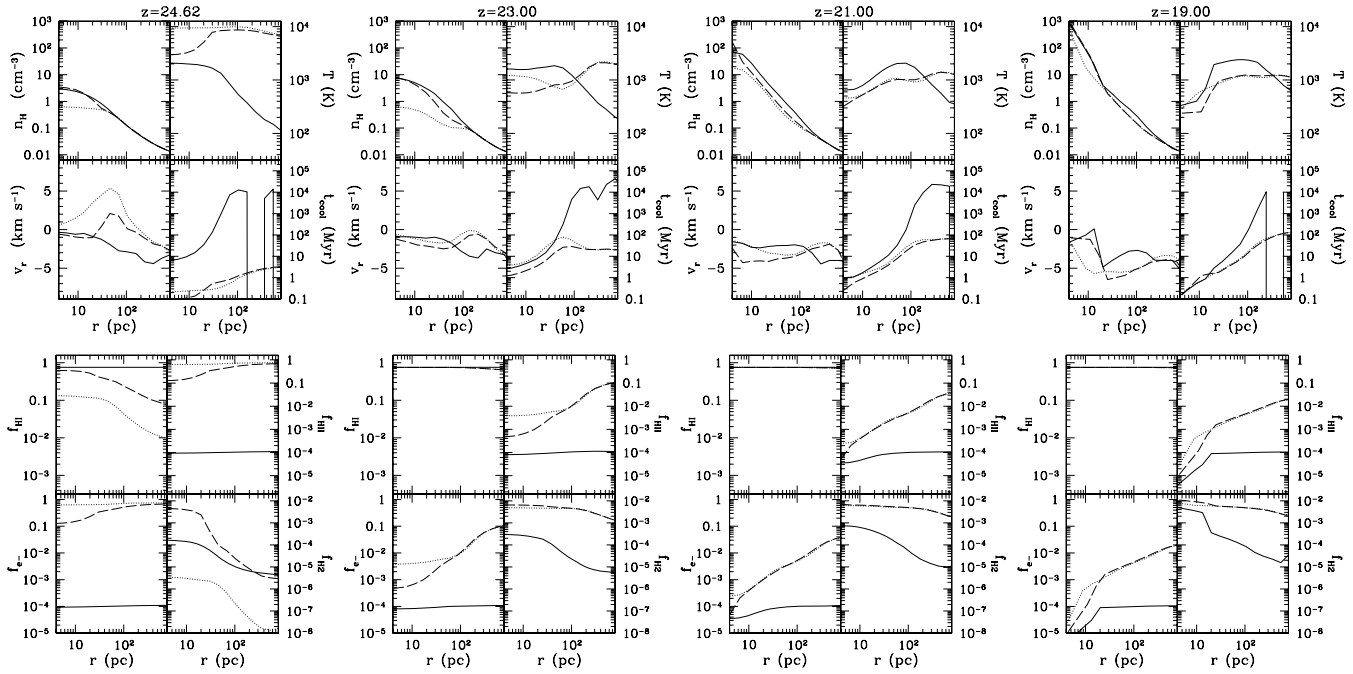

Figure 1. Spherically averaged radial profiles of the same halo in the NoUVB (solid lines), Heat0.08 (dashed lines) and Heat0.8 (dotted lines) simulation runs. This halo was first able to form CD gas at $z = 20$, 21, 19 in the NoUVB, Heat0.08 and Heat0.8 runs, respectively. The top and bottom pairs of the figures show snapshots at $z = 24.62$, 23, 21, 19 (left to right). The halo mass in the NoUVB run increases from $M = 4.2 \times 10^5\,\mathrm{M}_\odot$ at $z = 24.62$ to $M = 1.4 \times 10^6\,\mathrm{M}_\odot$ at $z = 19$. All quantities are shown in proper (not comoving) units. The upper panels show the hydrogen density, mass-weighted gas temperature, gas cooling time and radial velocity (clockwise from upper left). The bottom panels show mass fractions of H I, H II, H_2 and the number fraction of e^- (clockwise from upper left).

box.[1] Gas inside haloes which used to be at or close to hydrostatic equilibrium feels an increased pressure gradient from the rise in temperature, resulting in an outwards-moving pressure shock. Once the UVB is turned off, the gas quickly cools to $T \sim 10^3$ K through a combination of atomic, molecular hydrogen and Compton cooling. The molecular hydrogen formation time is shorter than the recombination time and a large amount of molecular hydrogen is produced, $x_{\mathrm{H_2}} \sim$ few $\times\, 10^{-3}$, irrespective of the density and temperature (see also Oh & Haiman 2002).[2] The pressure shock starts to dissipate and gas expelled from the centre of the halo starts falling back in (for a more complete description, readers are encouraged to see MBH06).

Quantitatively, we concluded that the net impact of a transient UVB on star formation could be understood simply in terms of the molecular hydrogen cooling time-scale:

$$t_{\mathrm{H_2}} = \frac{1.5 k_{\mathrm{B}} T}{\Lambda_{\mathrm{H_2}}} \frac{n_{\mathrm{g}}}{n_{\mathrm{H\,I}} n_{\mathrm{H_2}}} \tag{1}$$

$$\approx \frac{1.5 k_{\mathrm{B}} T}{\Lambda_{\mathrm{H_2}}} \frac{1}{n_{\mathrm{g}} x_{\mathrm{H_2}}}$$

$$\approx 4 \left(\frac{T}{10^3\,\mathrm{K}}\right)^{-2.5} \left(\frac{x_{\mathrm{H_2}}}{3 \times 10^{-3}}\right)^{-1} \left(\frac{n_{\mathrm{g}}}{1\,\mathrm{cm}^{-3}}\right)^{-1} \mathrm{Myr}, \tag{2}$$

Here, k_{B} is the Boltzmann constant; T is the temperature; $\Lambda_{\mathrm{H_2}}$ is the H_2 cooling function; x_{e} is the free electron number fraction; n_{g}, $n_{\mathrm{H\,I}}$ and $n_{\mathrm{H_2}}$ are the number densities of all baryons and electrons, neutral hydrogen and H_2, respectively; and the second equality is accurate shortly after $z_{\mathrm{UVB,off}}$, since the recombination times at high redshifts and inside haloes are very short.

We found that the net *delay* in star formation caused by the transient UVB is simply the ratio of the H_2 cooling time in the run with the UVB to the H_2 cooling time in the run without UV heating. This ratio is calculated near the halo core, shortly after the UVB disappears (when the shock first starts to dissipate and the gas behind it starts infalling again). For example, the delay in star formation of a halo in the Heat0.8 run with respect to the same halo in the NoUVB run is

$$f_{\mathrm{delay}} \sim \frac{t_{\mathrm{H_2}}^{\mathrm{Heat0.8}}}{t_{\mathrm{H_2}}^{\mathrm{NoUVB}}} \sim \left(\frac{T^{\mathrm{NoUVB}}}{T^{\mathrm{Heat0.8}}}\right)^{2.5} \left(\frac{n_{\mathrm{g}}^{\mathrm{NoUVB}}}{n_{\mathrm{g}}^{\mathrm{Heat0.8}}}\right) \left(\frac{x_{\mathrm{H_2}}^{\mathrm{Heat0.8}}}{x_{\mathrm{H_2}}^{\mathrm{NoUVB}}}\right)^{-1}. \tag{3}$$

We will now demonstrate that equation (3) is equally adept at quantifying feedback in our new simulations. First, we show the spherically averaged radial profiles of the same (typical) halo in the NoUVB (solid lines), Heat0.08 (dashed lines) and Heat0.8 (dotted lines) simulation runs in our Fig. 1. This halo, which has a mass of $4 \times 10^5\,\mathrm{M}_\odot$ at $z = 24.62$, was first able to form CD gas at $z = 20$, 21, 19 in the NoUVB, Heat0.08 and Heat0.8 runs, respectively. The top and bottom pairs of figures are snapshots at $z = 24.62$, 23, 21 and 19 (left to right). The upper panels show the hydrogen density, mass-weighted gas temperature, gas cooling time and radial velocity (clockwise from upper left). The bottom panels show mass fractions of H I, H II, H_2 and the number fraction of e^- (clockwise from upper left).

[1] It is important to note that we are operating in the optically thin limit; the accuracy and impact of that approximation are discussed in Section 5.

[2] Glover & Abel (2008) have recently shown that including cooling due to excitations of H_2 through collisions with protons and electrons can lead to a lower molecular hydrogen fraction by a factor of 2. This would result in a longer delay in star formation than shown here.

The profiles confirm the qualitative storyline from the beginning of this section. The outwards-moving pressure shock is evident in both UVB runs from the density and velocity panels at $z = z_{\rm UVB,off}$, just before the UVB was turned off. This gas has already cooled to $T = 10^3$ K and started to collapse back on to the halo only a few Myr afterwards at $z = 23$. Note that the outflow and the resulting suppression of gas near the core are stronger in the run with a stronger UVB. Haloes in the runs with a UVB also experience a strong boost in the H_2 fraction following $z_{\rm UVB,off}$, with the increase being insensitive to the strength of the UVB. Formation of CD gas in this halo is notably delayed until $z = 19$ in the Heat0.8 run, while being mildly expedited in the Heat0.08 run. Can this behaviour be understood through equation (3)? Let us focus on the output we have shortly after $z_{\rm UVB,off}$, at $z = 23$. We can note that at this redshift, the pressure-driven shock has almost dissipated and reached zero velocity with gas recommencing infall behind the shock. Plugging in appropriate values into equation (3) from the inner annulus of the halo, we obtain values of $f_{\rm delay} \approx 0.5$ and 1.5 for the Heat0.08 and Heat0.8 runs, respectively, in good agreement with the simulation outcomes. This behaviour again supports our conclusions in MBH06, where the same analysis held for a different, randomly chosen halo, and implies that we understand the physical picture associated with feedback in relic H II regions.

In order to quantify the suppression of CD gas by a transient UVB on our entire sample of haloes, we define (as in MBH06) the cumulative, fractional suppression of the number of newly formed haloes as

$$\delta_{N,\rm cd}(z) \equiv \frac{N_{\rm cd}^{\rm runi}(z) - N_{\rm cd}^{\rm runi}(z_{\rm UVB,on})}{N_{\rm cd}^{\rm NoUVB}(z) - N_{\rm cd}^{\rm NoUVB}(z_{\rm UVB,on})} - 1, \quad (4)$$

where $N_{\rm cd}^{\rm NoUVB}(z)$ and $N_{\rm cd}^{\rm runi}(z)$ are the total number of haloes with CD gas at redshift z in the NoUVB run and some given run i, respectively. This expression is well defined for $N_{\rm cd}^{\rm NoUVB}(z) > N_{\rm cd}^{\rm NoUVB}(z_{\rm UVB,on})$; for $N_{\rm cd}^{\rm NoUVB}(z) = N_{\rm cd}^{\rm NoUVB}(z_{\rm UVB,on})$, we set $\delta_{N,\rm cd}(z) \equiv 0$. Note that by definition, $N_{\rm cd}^{\rm NoUVB}(z_{\rm UVB,on}) = N_{\rm cd}^{\rm runi}(z_{\rm UVB,on})$.

Similarly, we define the cumulative, fractional suppression of the CD gas mass as

$$\delta_{M,\rm cd}(z) \equiv \frac{M_{\rm cd}^{\rm runi}(z) - M_{\rm cd}^{\rm runi}(z_{\rm UVB,on})}{M_{\rm cd}^{\rm NoUVB}(z) - M_{\rm cd}^{\rm NoUVB}(z_{\rm UVB,on})} - 1, \quad (5)$$

where $M_{\rm cd}^{\rm NoUVB}(z)$ and $M_{\rm cd}^{\rm runi}(z)$ are the total mass of CD gas at redshift z in the NoUVB run and some given run i, respectively. The total CD gas mass is obtained by merely summing the CD gas masses for all of the haloes in the simulation. As for equation (4), this expression is well defined for $M_{\rm cd}^{\rm NoUVB}(z) > M_{\rm cd}^{\rm NoUVB}(z_{\rm UVB,on})$, and for $M_{\rm cd}^{\rm NoUVB}(z) = M_{\rm cd}^{\rm NoUVB}(z_{\rm UVB,on})$, we set $\delta_{M,\rm cd}(z) \equiv 0$.

Equations (4) and (5) provide an estimate of how the CD gas has been affected by the presence of a UVB, *following* the turn-on redshift of the UVB, $z_{\rm UVB,on}$ (the values at $z_{\rm UVB,on}$ are subtracted in order to provide a more sensitive measure of *relative* changes of CD gas). As defined above, $\delta_{N,\rm cd}(z) = 0$ and $\delta_{M,\rm cd}(z) = 0$ if the UVB has no effect. If the effect of a UVB is positive, resulting in positive feedback, $\delta_{N,\rm cd}(z)$ and $\delta_{M,\rm cd}(z)$ would be positive. If the effect of the UVB is negative, $\delta_{N,\rm cd}(z)$ and $\delta_{M,\rm cd}(z)$ would be negative.

In Fig. 2, we plot the values of $M_{\rm cd}^{\rm runi}(z)$ (top panel) and $N_{\rm cd}^{\rm runi}(z)$ (bottom panel) in our four simulation runs with no LWB: run i = NoUVB (crosses), Flash (dashes), Heat0.08 (triangles) and Heat0.8 (squares). We note that the number of haloes with CD gas increases in all runs until $z \sim 15$, when our central refined regions start becoming more non-linear. At these lower redshifts, haloes become contaminated with large DM particles entering from outside the refined region and we remove them from our analysis sample (see Section 2).

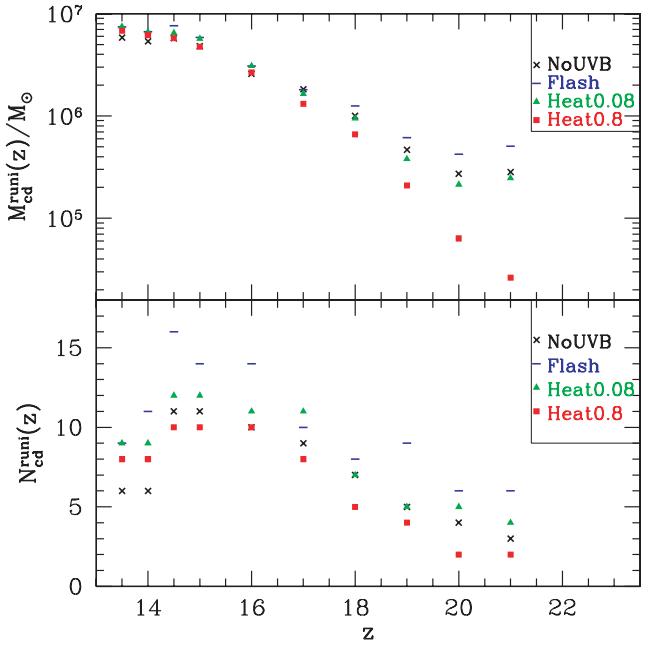

Figure 2. Values of $M_{\rm cd}^{\rm runi}(z)$ (top panel) and $N_{\rm cd}^{\rm runi}(z)$ (bottom panel) as defined in equations (5) and (4), respectively. The results are displayed for the NoUVB (crosses), Flash (dashes), Heat0.08 (triangles) and Heat0.8 (squares) simulation runs.

The corresponding values of $\delta_{M,\rm cd}(z)$ and $\delta_{N,\rm cd}(z)$ are plotted in Fig. 3 in the top and bottom panels, respectively. Although some of the notable fractional changes shown in Fig. 3 might appear statistically insignificant due to the small number statistics inferred from Fig. 2, it should be noted that these runs are not uncorrelated

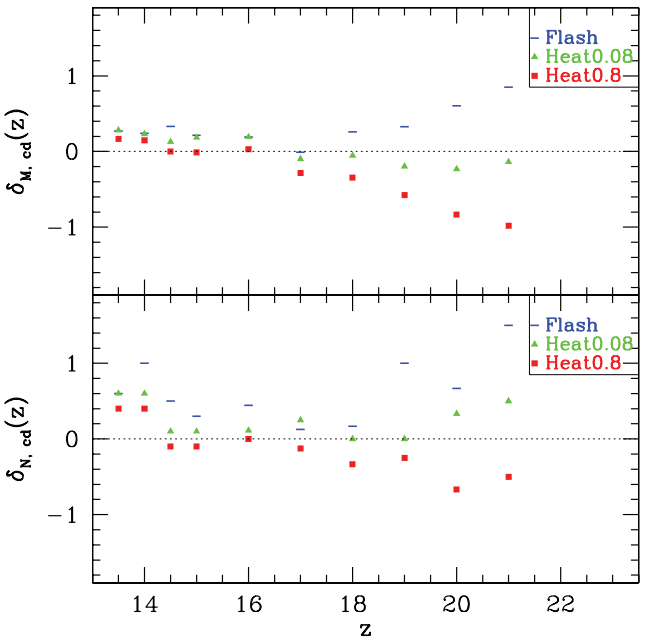

Figure 3. Values of $\delta_{M,\rm cd}(z)$ (top panel) and $\delta_{N,\rm cd}(z)$ (bottom panel) as defined in equations (5) and (4), respectively. The results are derived from Figure 2 and displayed for the Flash (dashes), Heat0.08 (triangles) and Heat0.8 (squares) simulation runs.

experiments. In other words, each of our runs in Table 1 is seeded with the same initial conditions, and so small relative changes compared to the NoUVB run are significant (i.e. the errors are not Poisson). Nevertheless, there are some minor differences between the runs in the amount of 'contamination' by DM particles outside of our refined region.

In MBH06, we presented two main inferences regarding the effects of a transient UVB (aside from the delay due to cooling times discussed above): (1) a 'critical' background value of $J_{21}^{\rm UV} \sim 0.1$ separated positive from negative feedback (stronger backgrounds result in negative feedback, while weaker backgrounds result in positive feedback; see the discussion surrounding equation 3 above) and (2) the feedback effects, regardless of the sign, were transient and started to 'disappear' by $z \sim 18$. However, we were unable to evolve our simulations below $z < 18$, since the central refined region became too non-linear and further progress was computationally prohibitive. Thus, point (2) was an inference based on a figure analogous to Fig. 3.

In this work we present results from a less biased region and are able to go to lower redshifts, $z \sim 13.5$. Thus, we can test both of the above conclusions and see if they are sensitive to the large-scale halo environment and redshift. From Fig. 3, we see that *both* conclusions are valid for these simulations as well. In other words, our transient (corresponding to the expected lifetime of a Pop III star) UVB results in transient feedback which disappears after ∼30 per cent of the Hubble time, with $J_{21}^{\rm UV} \sim 0.1$ separating net positive and negative feedback. Thus, these conclusions seem to be fairly insensitive to the large-scale overdensity of the simulated region and by extension to the redshift-dependent properties of haloes at $z_{\rm UVB,on}$.

It is important to note a new result evident in Fig. 3: all runs with a transient UVB experience eventual positive feedback at $z \lesssim 15$. This is true regardless of the strength of the UVB. We will examine this interesting result further in Section 4.

3.1 Adding a persistent Lyman–Werner background

Next, we investigate how the combination of transient UV heating and a persistent LWB impacts star formation. This is a more physically relevant scenario, since an LWB is likely established before a large fraction of the Universe has been reionized (Haiman et al. 2000).

Photons in the LW band dissociate H_2 molecules; thus by definition they provide additional negative feedback, undercutting some of the enhancement in the H_2 abundances in relic H II regions. Negative feedback from an LWB kicks in when the H_2 dissociation time-scale becomes shorter than the H_2 formation time-scale. Since the formation time-scale is inversely proportional to gas density, whereas the dissociation time-scale is independent of density, the density decrease caused by UV heating should make haloes more susceptible to the negative feedback of an LWB (Oh & Haiman 2003).[3] We investigate these processes further below.

Specifically, in Fig. 4, we plot values of $\delta_{M,\rm cd}(z)$ (top panel) and $\delta_{N,\rm cd}(z)$ (bottom panel) for our runs including an LWB. The LWB turns on at $z = 24.62$ and remains on. At the simplest level, we can see the suppression of molecular hydrogen (and hence cooling)

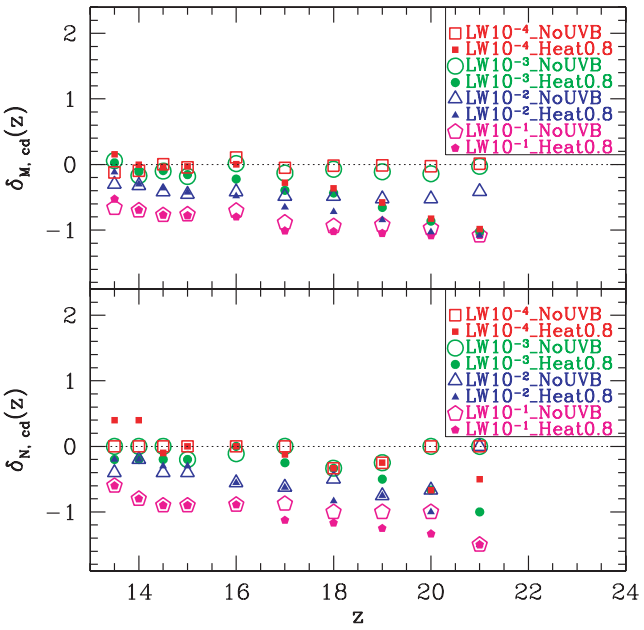

Figure 4. Suppression of cold dense gas in haloes in simulations runs that include a persistent LWB. The LWB had specific intensities of $J_{\rm LW} = 10^{-4}$, 10^{-3}, 0.01 or 0.1 (normalized at 12.87 eV, in units of 10^{-21} erg s^{-1} cm^{-2} Hz^{-1} sr^{-1}). Each of these three LWBs is applied to both our NoUVB and Heat0.8 runs at $z = 24.62$, and is subsequently left on. Values of $\delta_{M,\rm cd}(z)$ (top panel) and $\delta_{N,\rm cd}(z)$ (bottom panel) are shown, as defined in equations (5) and (4), respectively.

due to the LWB by the more negative values of both $\delta_{M,\rm cd}(z)$ and $\delta_{N,\rm cd}(z)$ at a fixed redshift.

Does this panel show evidence for the *additional* negative impact of the transient UVB discussed above? Without UV heating, an LWB with a specific intensity of $J_{21}^{\rm LW} = 0.01$ is needed for notable negative feedback (see the blue empty triangles at $z \leq 14$ in the lower panel). This value is similar to the one found in MBH06, where we showed that by equating H_2 cooling and H_2 photodissociation one expects this critical LWB to scale as $J_{21}^{\rm LW} \propto n_{\rm g} f_{\rm H_2}/T$.[4] When the UV heating is added, this critical value of $J_{21}^{\rm LW}$ causing negative feedback decreases by a factor of ∼10 to $J_{21}^{\rm LW} \sim 10^{-3}$ (see the green solid circles in the lower panel at $z \leq 14$). This decrease seems to confirm the above arguments. However, such an interpretation is too simplistic and the negative impact of the LWB can be ameliorated by positive feedback inside the H II region at lower redshifts, as we shall see in Section 4.

From Fig. 4, one can also note that a value of $J_{21}^{\rm LW} \sim 10^{-3}$–$10^{-2}$ separates feedback regimes dominated by an LWB from those dominated by our transient UVB. This can be seen by the fact that the amount of suppression differs between the NoUVB and Heat0.8 cases at low values of the LWB (i.e. for $J_{21}^{\rm LW} < 10^{-3}$), while at large values of $J_{21}^{\rm LW}$, the amount of suppression is independent of the UVB. Near the threshold value of $J_{21}^{\rm LW}$, negative feedback transitions from being UV heating dominated (at $z \gtrsim 17$, or $\lesssim 100$ Myr after $z_{\rm UVB,off}$) to being LWB dominated ($z \lesssim 17$, or $\gtrsim 100$ Myr after $z_{\rm UVB,off}$). As highlighted in MBH06, this 'transition' behaviour can be understood as the combined result of two effects: the UV heating

[3] Note that the temperature increase associated with a UVB does not contribute much to this combined negative feedback because the ionized gas is able to Compton-cool down to the virial temperatures of these minihaloes.

[4] Since the mean density of gas collapsing into haloes in these simulations is less than a factor of 2 smaller than those in MBH06, we roughly expect this critical value of $J_{21}^{\rm LW}$ to also be less than a factor of 2 smaller (at least in the linear regime).

is turned off and its impact is transient, while the critical LWB scales roughly with the inverse of the density (Haiman et al. 2000; Oh & Haiman 2003) and hence a fixed LWB will have a larger impact at lower densities or decreasing redshifts.

4 EVENTUAL POSITIVE FEEDBACK

So far, we have not focused on the interesting new result hinted by the previous figures (e.g. see the $z \lesssim 14.5$ points in Fig. 3). This figure shows evidence of delayed (approaching our lowest redshifts) *positive* feedback in *all* runs with a UVB. This result is somewhat surprising given that the Heat0.8 run shows strong negative feedback initially after $z_{\rm UVB,off}$. In fact, as was already pointed out when discussing Fig. 3, the initial feedback, whether positive or negative, fades away in *all* runs by $z \sim 17$.

In Fig. 5, we show the total gas fractions (top panels) and CD gas fractions (bottom panels) from haloes at $z = 13.5$. The positive feedback mentioned above is immediately evident from this figure, and shows explicitly the masses of the affected haloes. In particular, the NoUVB run at $z = 13.5$ has three *fewer* haloes hosting CD gas than the Flash and Heat0.08 runs, and two *fewer* than even the Heat0.8 run (see also Fig. 2). These are some of the smallest and youngest of such haloes at these redshifts. We also verify that these haloes formed in less biased and less overdense regions than the haloes which did not experience such positive feedback.

What is the physical cause of such delayed positive feedback? Before we attempt to answer this question, let us briefly review the sequence of feedback-related events arising from a transient UVB.

(i) When the UVB turns on, gas gets ionized and heated to temperatures $\gtrsim 10^4$ K.

(ii) The temperature increase sets off an outwards-moving pressure shock in the cores of haloes, where density profiles have already steepened as gas approached hydrostatic equilibrium. This pressure shock smooths out the gas distribution and leads to a decrease in gas density in the cores of haloes.

(iii) Once the UVB is turned off, the gas rapidly cools to $T \sim 10^3$ K through a combination of atomic, molecular hydrogen and Compton cooling. This temperature approximately corresponds to the gas temperature at the virial radius of such a protogalactic, molecularly cooled halo, thus effectively neutralizing the impact of temperature change on feedback.

(iv) A large amount of molecular hydrogen is produced, $x_{\rm H_2} \sim$ few $\times\, 10^{-3}$, irrespective of the gas density and temperature.

(v) The pressure-shock begins to dissipate and gas with a newly enhanced H_2 abundance starts falling back on to the partially evacuated halo.

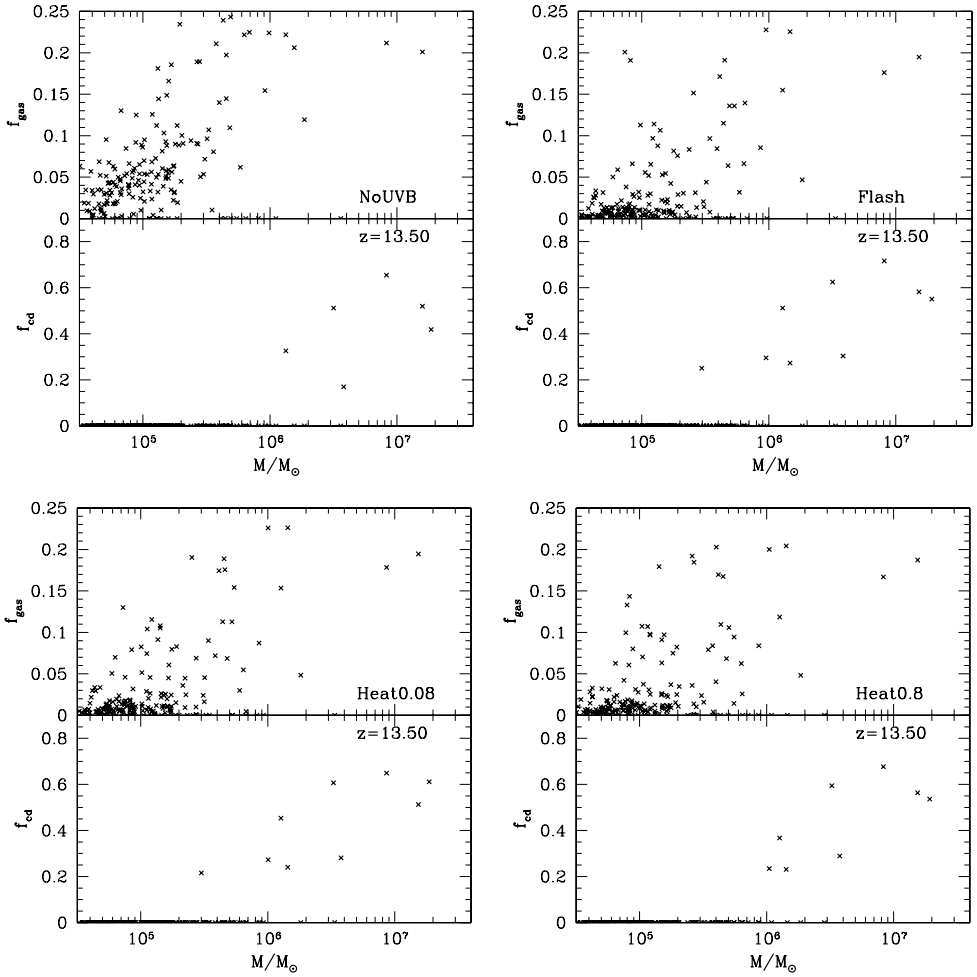

Figure 5. Total gas fractions (top panels) and cold, dense gas fractions (bottom panels) as a function of the total halo mass at redshift $z = 13.5$, the lowest redshift output of our simulations. The four panels correspond to the NoUVB (top left), Flash (top right), Heat0.08 (bottom left) and Heat0.8 (bottom right) simulation runs. Note that all runs with a UVB have more haloes with CD gas than the NoUVB run.

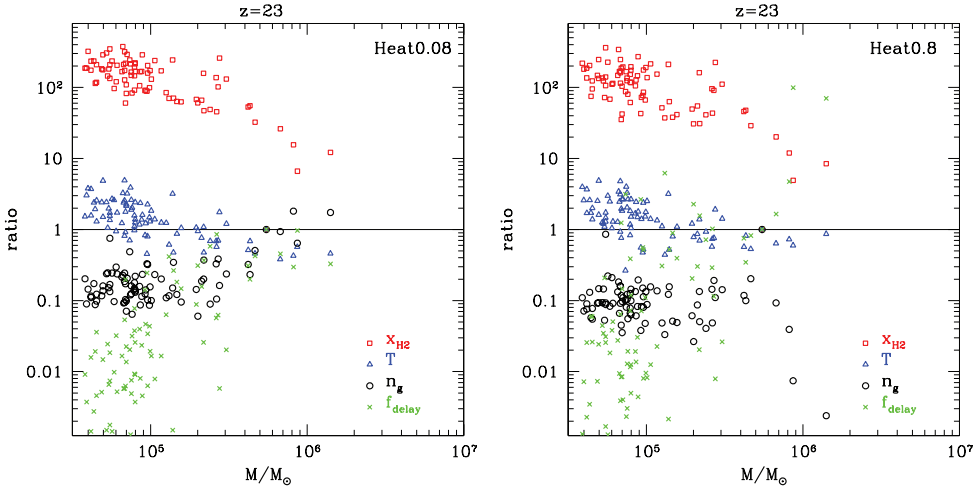

Figure 6. Ratio of the H_2 fractions (red squares), the temperatures (blue triangles) and the average gas densities (black circles) within the central 15 pc (proper) of haloes. Ratios of these quantities in the Heat0.08 and Heat0.8 runs over the fiducial NoUVB run are shown in the left-hand and right-hand panels, respectively, at $z = 23$. The delay factors from equation (3) are also plotted as green crosses.

It is the balance between the density depletion in step (ii) (which is dependent on the UVB intensity) and the enhanced cooling capability of the gas from step (iv) (which is independent of the UVB intensity), which determines the transient feedback outcomes discussed in Section 3. But what happens to gas which is not in the cores of already formed haloes with a steepened density profile? In the extreme case of homogeneous gas, the UVB-induced temperature increase in (i) does not translate into a pressure shock. Thus, there is no density depletion from step (ii). In the more realistic case of a clumpy gas distribution, pressure gradients will still form and smooth out the gas distribution, but the resulting depletion will be less than in the cores of haloes in hydrostatic equilibrium. However, such lower density gas outside of haloes will still be able to cool to temperatures of $\sim 10^3$ K since the Compton cooling time is independent of density, and at these high redshifts is over a factor of 2 shorter than the recombination time at mean density [in fact, these lower density regions take longer to recombine and hence can Compton-cool for a longer period reaching lower temperatures (Oh & Haiman 2002); see also equations 2 and 3 in MBH06]. Likewise, step (iv) mentioned above also applies to such lower density gas, with the transient background resulting in an enhanced molecular hydrogen abundance. Thus, we expect gas which has not yet formed a self-similar (e.g. Navarro, Frenk & White 1996) halo profile to experience weaker negative feedback [i.e. step (ii)], and the same amount of positive feedback [i.e. step (iv)], when exposed to identical transient UVBs.

This conclusion is perhaps a bit counterintuitive, since many cosmological radiative feedback studies find that feedback is a strong function of halo mass, with more massive, earlier forming haloes being *less* susceptible to negative feedback (Efstathiou 1992; Barkana & Loeb 1999; Gnedin 2000; Kitayama & Ikeuchi 2000; Shapiro et al. 2004; Dijkstra et al. 2004; Mesinger & Dijkstra 2008). However, there are two important distinctions here: we are discussing feedback resulting from a *transient* UVB and we are comparing haloes which have not yet formed and set up a self-similar gas profile at $z_{\rm UVB,off}$ to those which have already formed, rather than comparing *within* each of these two groups.

We also see some evidence of these trends in Fig. 6, where we plot the ratio (in runs with a UVB over the fiducial NoUVB run) of the H_2 fractions (red squares), the temperatures (blue triangles) and the average gas densities (*black circles*) within the central 15 pc (proper) of haloes. These quantities are shown shortly after $z_{\rm UVB,off}$, at $z = 23$. As already noted in Section 3 and in (iv) above, the H_2 fraction tends to increase by the same factor, regardless of the nature of the heating. As a result, the sign of the overall feedback (negative or positive) is determined primarily by whether or not the depression of the gas density overcomes the positive effects of this H_2 enhancement. The density depletion does depend strongly on the type and amount of heating. This depletion, shown in black circles, is of course stronger for the Heat0.8 than the Heat0.08 run. Thus haloes in the former initially experience strong negative feedback and in the latter negligible or weak positive feedback, as we have seen in Section 3 and as noted by the green crosses in the figure. Note however that the difference in the amount of gas depletion between these two heating runs decreases with decreasing halo mass as one begins being affected by Jeans/filtering scale effects.[5] Following the above argument, this trend should continue and density depletion should decrease in regions which are less evolved (i.e. the black points should approach unity as the halo mass is decreased below the values shown in the figure). It is these regions which become the progenitors of our haloes experiencing eventual positive feedback. Unfortunately, at $z = 23$, these regions are too unevolved to be identified by our halo finding algorithm and thus do not appear in Fig. 6.

This eventual positive feedback should be quite sensitive to the LWB. Indeed, looking at the bottom panel of Fig. 4, we see that this feedback effect is wiped out if $J_{21}^{\rm LW} \gtrsim 10^{-3}$. It is likely that such modest values of $J_{21}^{\rm LW}$ are reached well before the majority of the Universe is ionized (Haiman et al. 2000), though the build-up of the LWB can be slowed by an increasing optical depth to LW photons from the enhanced H_2 abundances in relic H II regions (Johnson, Greif & Bromm 2007) or in shells surrounding H II regions (Ricotti, Gnedin & Shull 2001; Kuhlen & Madau 2005; though see Kitayama et al. 2004). Thus, studying the true physical importance

[5] Note that accurately modelling Jeans smoothing requires very high resolution in both DM and gas (Naoz, Barkana & Mesinger 2009). These small scales are shown in Fig. 6 merely to show qualitative trends.

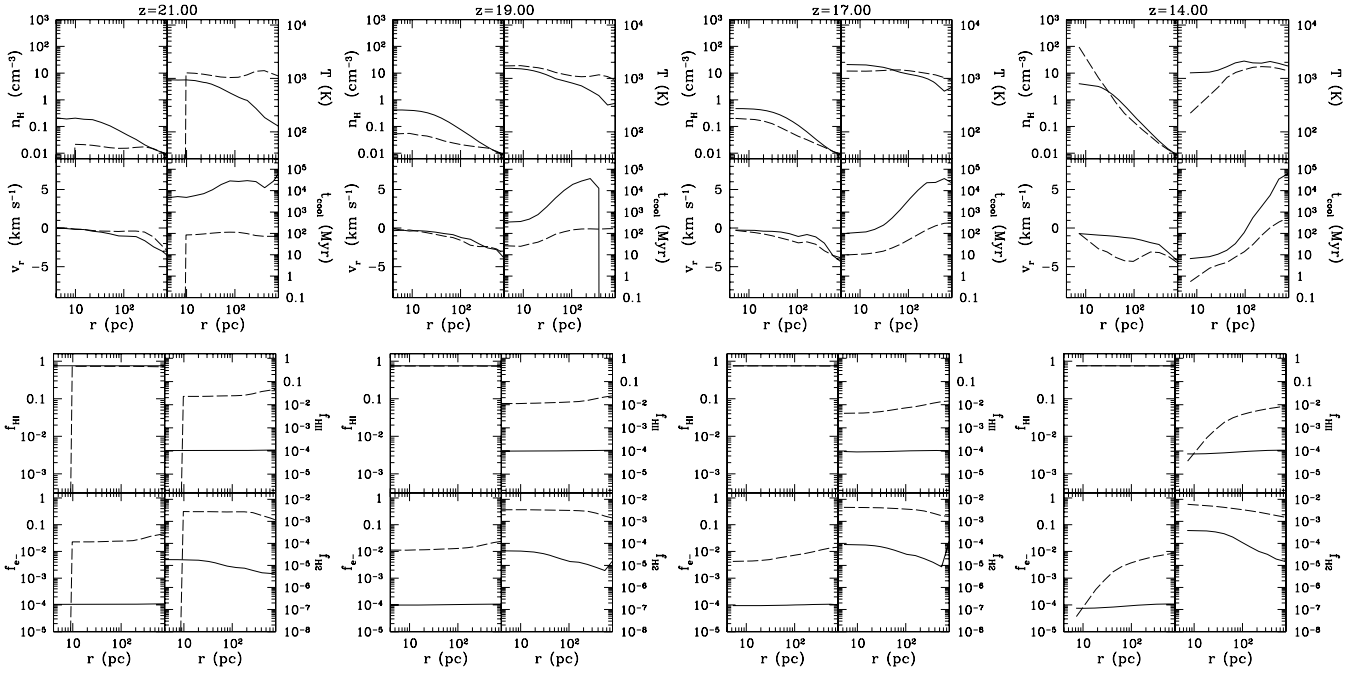

Figure 7. The same quantities as in Fig. 1, but for a halo which experiences positive feedback in the Heat0.8 run. Solid and dashed curves correspond to the NoUVB and Heat0.8 runs, respectively.

of this positive feedback mechanism would have to be done with self-consistent cosmological simulations of reionization.

Now, let us look at specific examples by studying the evolution of one such halo experiencing eventual positive feedback. In Fig. 7, we plot the same quantities as in Fig. 1, but for a halo which experiences positive feedback in the Heat0.8 run. Note that, unlike the more evolved haloes which are subjected to the transient feedback and have already formed at $z_{\rm UVB,off}$, the earliest snapshot we have of this halo is at $z = 21$. Solid and dashed curves correspond to the NoUVB and Heat0.8 runs, respectively.

It is important to note that this halo forms considerably after $z_{\rm UVB,off}$, and thus the 'density depletion' seen in the figure at $z \gtrsim 17$ is of a different nature than discussed in Section 3 and Fig. 1. Namely, this gas was not evacuated from the halo centre with a pressure shock. Instead, these late-forming haloes start pulling in baryons when their virial temperature exceeds that of the gas temperature. The heating and subsequent Compton cooling following the transient UVB set the intergalactic medium (IGM) gas temperature in these runs at $T \sim 10^3$ K. Thus, baryonic infall on to newly formed haloes can commence when $T_{\rm vir} \gtrsim 10^3$ K. Since the IGM is cooler in the NoUVB run, gas there gets a 'head-start' in accreting on to DM haloes. However, as is evident in the figure, the enhanced H_2 cooling channel in the Heat0.8 run allows the gas to quickly catch up and surpass its twin in the NoUVB run. Thus by redshift $z = 14$, the halo has formed CD gas in the Heat0.8 run, but not in the NoUVB run.

How does adding an LWB impact this positive feedback? From Fig. 4, we have already surmised that a background intensity of $J_{21}^{\rm LW} \gtrsim 10^{-3}$ can offset these trends by decreasing the enhanced H_2 fraction in relic H II regions. In Fig. 8, we plot profiles from the same halo in the LW10^{-3}_NoUVB (solid curves) and LW10^{-3}_Heat0.8 (dashed curves) runs. By comparing the solid curves from Fig. 7 to the dashed curves from Fig. 8, one confirms that an LWB with $J_{21}^{\rm LW} \sim 10^{-3}$ effectively neutralizes the positive feedback from the transient UVB. Thus at $z = 14$, the halo core has a similar gas profile and cooling time in the NoUVB and LW10^{-3}_Heat0.8 runs.

By comparing the two profiles at $z = 14$ in Fig. 8, we see that the transient UVB still stimulates positive feedback, but the effect is not nearly as dramatic. Specifically, in the halo core at $z = 14$ the density is enhanced and the cooling time is lowered (both by a factor of $\sim$2) in the LW10^{-3}_Heat0.8 run compared to the LW10^{-3}_NoUVB run. This level of positive feedback is much more modest compared with the case with no LWB, where the equivalent density enhancement was a factor of $\sim$50 and the cooling time was lower by a factor of $\sim$15 (see Fig. 7).

Does this trend continue as we increase the strength of the UVB? In Fig. 9, the solid and dashed curves correspond to the LW10^{-2}_NoUVB and LW10^{-2}_Heat0.8 runs at $z = 14$, respectively; similarly in Fig. 10, the solid and dashed curves correspond to the LW0.1_NoUVB and LW0.1_Heat0.8 runs at $z = 14$, respectively. Here we see that the core density in the LW0.1_Heat0.8 run is lower than in the LW0.1_NoUVB run, but the cooling time is *also lower* by the same factor of $\sim$2 seen in Fig. 8, sourced by the enhanced H_2 fraction. In fact, from higher redshift output and the previous figures, we see that the density is still 'catching up' as time progresses, namely the dashed density curve keeps getting closer to the solid density curve. Thus we see that haloes inside relic H II regions, when exposed to the same LWB, always have a higher H_2 abundance and shorter cooling times than haloes outside relic H II regions, allowing gas to cool faster once it finally begins to collapse on to the halo.

It is important to note that in this regime where a strong LWB dominates the overall feedback, star formation is likely to be substantially delayed. This delay can be long enough to allow the halo to be photoevaporated during reionization, before it had a chance to host additional stars. Thus if one is only concerned with the fate of those minihaloes contributing their ionizing photons to the progress of reionization, it is possible that the sole *persistent* feedback mechanism is *positive*.

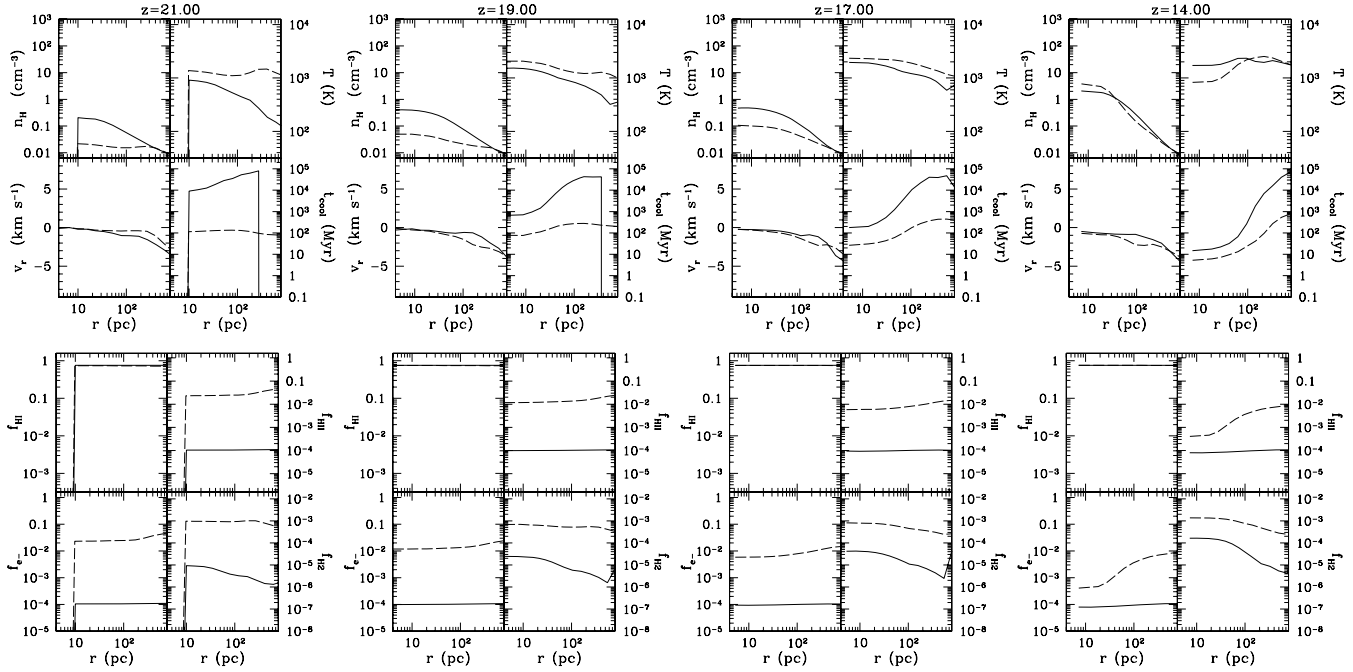

Figure 8. Same as Fig. 7, but with solid and dashed curves corresponding to the LW10^{-3}_NoUVB and LW10^{-3}_Heat0.8 runs, respectively.

5 THE IMPACT OF NEGLECTING RADIATIVE TRANSFER

As we have noted a number of times in this paper, our simulations assume the optically thin limit, for both ionizing radiation and photodissociating LW photons. Both of these approximations clearly fail at points in our simulations, and so it is necessary to understand the nature and implications of this approximation. For clarity, we discuss ionizing photons and LW photons separately.

We discuss the impact of radiation hydrodynamic (RHD) effects due to ionizing photons first. There is now a substantial body of literature on the ionization of primordial gas haloes (Shapiro et al. 2004; Whalen, Abel & Norman 2004; Iliev et al. 2005; Alvarez et al. 2006; Susa & Umemura 2006; Abel et al. 2007; Whalen et al. 2008; Wise & Abel 2008b) and the broad outline of how haloes are ionized is now well understood. We begin by noting that the optical depth of the haloes which are ionized in our simulation box at $z = 25$ (as shown in Fig. 1), as measured from the virial radius to the centre, is – at the Lyman limit – well over 100. Therefore, at first blush, the optically thin limit seems like a poor approximation. However, this impression is not entirely accurate for two reasons.

First, we are studying the *later* formation of haloes in relic H II regions, and much of the gas that eventually falls into a halo at late times is *not* in the centre of haloes at reionization. This is the question that Oh & Haiman (2003) asked: does the excess entropy generated in low-density gas in relic H II regions prevent it from forming stars at later times. This low-density gas has much lower optical depth and so is very likely to be ionized by a nearby Pop III star.

Second, even for the gas in the centres of our haloes at $z_{\rm UVB,on}$, the optically thin approximation is not as bad as the large optical depth at the Lyman limit indicates. We can see this more clearly by comparing our results to RHD calculations. For example, take the (typical) halo shown in Fig. 1. The central density when ionization begins (at $z = 25$) is just slightly over 1 cm^{-3}. This value is much below the central density (10^4 cm^{-3}) assumed by Susa & Umemura (2004), and is not that different from their critical density for self-shielding (depending on the assumed distance of the source). A better comparison is with the '023' series of simulations run in Whalen et al. (2008), which have almost identical central densities. As is shown in fig. 17 of that paper, this halo is disrupted and dissociated for all assumed distances of the first star. Comparing figs 9 and 10 of that paper to our Fig. 1 shows some obvious differences due to radiative transfer effects, but the basic evolution is not all that different. In particular, after a few Myr, the density at the halo centre has decreased by about a factor of $\sim$5 after $\sim$3 Myr, while the molecular hydrogen fraction has increased to a few times 10^{-3}. These numbers are very similar to what we find, and it is these basic facts which, we argue, cause the delay in future star formation, as discussed earlier. The reason for the similarity is that, as it sweeps over the halo, the ionization front can quickly ionize hydrogen until it transitions to a D-type front and stalls. However, this happens only $\sim$15 pc from the core, at densities slightly below 1 cm^{-3}, and the shock generated by the D-type front quickly disperses the core.

Of course, we do not claim to reproduce the RHD in detail. For example, we do not reproduce the thin self-shielded filament at the lower right of fig. 10 of Whalen et al. (2008) nor do we follow the detailed shock compression or 'rocket' offset of the core. However, by choosing to apply the ionizing flux at a redshift when the haloes have low masses and central densities, we minimize the impact of the radiation transfer. To verify that this is actually true in our simulations, we examined the central densities and masses of our haloes at $z = 25$; we find that all haloes except for one have masses below 10^6 M$_\odot$ and central densities below $\sim$2 cm^{-3} (one halo has $M > 10^6$ M$_\odot$ and $n_c = 7 \times 10^3$ cm^{-3}). Our halo abundance is consistent with predictions from the conditional Press–Schechter formalism (MBH06). We chose this approach because we are interested in investigating the impact of relic H II regions on the formation of structure which forms significantly later, rather than studying the impact of a Pop III star on a nearby, highly collapsed halo. In particular, as noted in the introduction, our motivation is to follow up on the suggestion of Oh & Haiman (2003) that relic

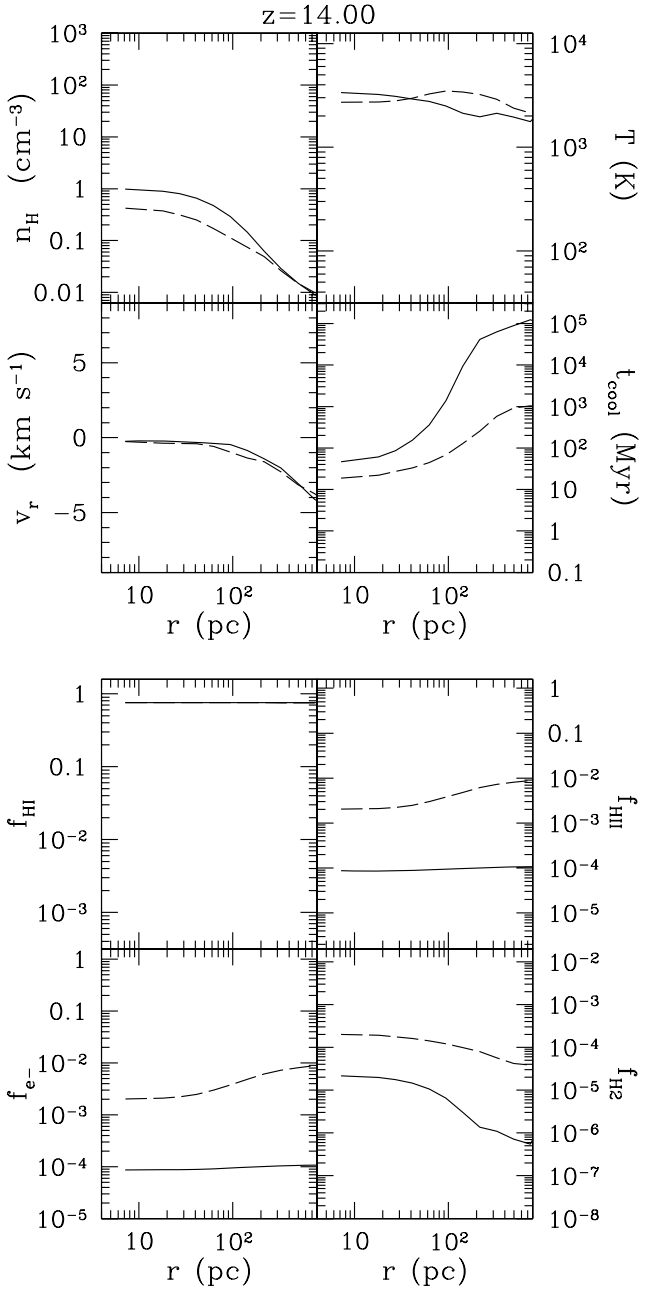

Figure 9. Same as Fig. 7, at $z = 14$, but with solid and dashed curves corresponding to the LW10^{-2}_NoUVB and LW10^{-2}_Heat0.8 runs, respectively.

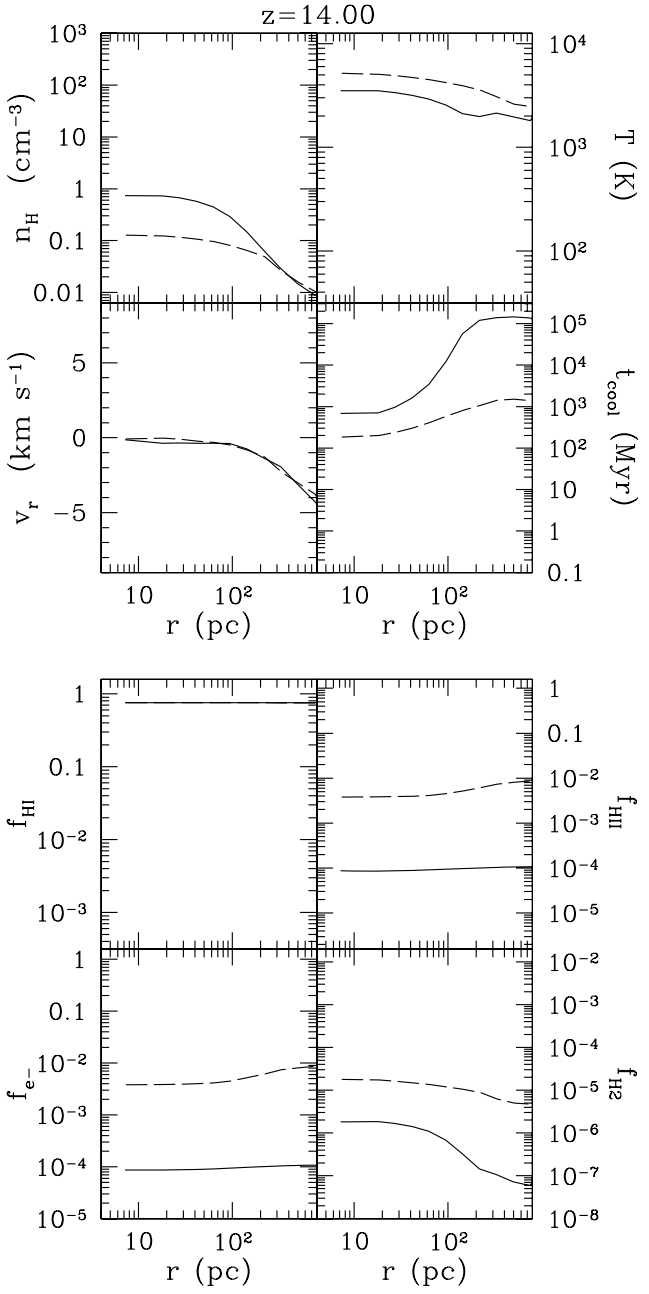

Figure 10. Same as Fig. 7, at $z = 14$, but with solid and dashed curves corresponding to the LW0.1_NoUVB and LW0.1_Heat0.8 runs, respectively.

H II regions will imprint an excess entropy on the low-density gas at early times, which will then suppress later star formation. Of course, we stress that it is still important to examine our results with a more realistic RHD treatment.

The results discussed in the section on positive feedback (Section 4) are even more robust because in that case the haloes form out of gas that was barely overdense when the ionization occurred. As can be seen in Fig. 7, even at $z = 21$ (long after the transient ionization), the central density of the halo (in the NoUVB case) is only $0.2\,\mathrm{cm}^{-3}$.

Another useful comparison of our results can be made with Wise & Abel (2008a), who used a full cosmological simulation of Pop III star formation including radiative transfer (albeit in a region considerably smaller than considered there). While a direct comparison is difficult because Wise & Abel (2008a) do not explicitly measure the suppression due to photoionization, a number of conclusions can be drawn. First, it is clear from fig. 7 of that paper that they also see the evaporation of gas from low-mass haloes and filaments, and the resulting density field in the two simulations looks remarkably similar. In addition, the time difference between the first Pop III object and the formation of the second is about 80 Myr, consistent with the time delay derived in this paper. On the other hand, one important point that comes out of that paper is that, because Pop III star formation tends to be clustered, relic H II regions do not sit isolated for longer periods of time and so a region of space may undergo multiple ionization episodes, something which is not considered in this work.

Next, we turn to LW photons. First, we remind the reader that we are discussing a persistent LWB, and that although the LW flux is produced by the same *class* of objects that generate the transient UV flux, it is not produced by the same physical objects. As discussed in more detail in Haiman et al. (1996), the LWB is accumulated from a large number of distant sources. The effective optical depth in the LW lines in the background IGM, over a Hubble distance, is at most $\tau \approx 1$–2 (Haiman et al. 2000; Ricotti et al. 2001), so the Olbers integral for the LWB is dominated by the large number of sources at a good fraction of the Hubble distance. In comparison, the ionizing photons come exclusively from the much fewer source(s) nearby, within the local H II region.

LW photons can be self-shielded by a sufficient column of H_2. Here again, there are two regimes. One is the large quantities of low-density gas in the relic H II regions that form substantial amounts of molecular hydrogen immediately after the ionizing flux is turned off (e.g. Kuhlen & Madau 2005). Although H_2 formed in this manner may slow the build-up of a persistent LWB, it does not – for a given LWB – provide a large amount of shielding. For example, Johnson et al. (2007) find typical values of LW optical depths of the order of unity for a single relic H II region. This means that the LW flux inside the relic H II region can be reduced by a factor of a few, but it also means that it does not take long for the persistent LWB to 'burn off' the H_2 produced in relic H II regions.

The second regime occurs after the ionized gas falls back into the collapsed haloes, where H_2 is in equilibrium between formation and photodestruction. In this case, when a sufficient column density of H_2 is formed, it can effectively attenuate the LW flux. Based on our simulations, we find that when CD gas forms, the LW optical depth can be of the order of unity or larger, indicating that self-shielding can play a role during the recollapse (although probably not during the photoionization process itself). Therefore, we caution readers that the critical LW values we give above may need to be increased when self-shielding is properly accounted for.

Finally, we note that in simulations with full radiative transfer, the photoionizing flux can also vary across a given halo (relic H II regions have radii of 2–3 kpc, while the Lagrangian radius of a typical halo in our simulations is of the order of 0.5 kpc). This also means that, while most forming haloes lie either completely inside or outside a relic H II region, some protohaloes could be partially ionized.

6 CONCLUSIONS

UV radiation from early astrophysical sources could have a large impact on subsequent star formation in nearby protogalaxies and in general on the progress of cosmological reionization. Theoretical arguments based on the absence of metals in the early Universe suggest that the first stars were likely massive, bright, yet short-lived, with lifetimes of a few million years. Here we study the impact of the transient radiation arising from such stars on early protogalaxies. We apply the same statistical approach as in MBH06, studying various combinations of transient UVBs and persistent LWBs, using the hydrodynamical simulation code, ENZO. We also study a more typical and relevant region whose protogalaxies form at lower redshifts, $z \sim 13$–20. This allows us to trace feedback effects on longer time-scales and lower redshifts.

We confirm the results of MBH06 that feedback in the relic H II regions resulting from such transient radiation is itself transient. Feedback effects dwindle away after ∼30 per cent of the Hubble time, and the same critical specific intensity of $J_{\rm UV} \sim 0.1 \times 10^{-21}\,{\rm erg\,s^{-1}\,cm^{-2}\,Hz^{-1}\,sr^{-1}}$ separates positive and negative feedback regimes. A weaker UVB stimulates subsequent star formation inside the relic H II regions, by enhancing the molecular hydrogen abundance. A stronger UVB delays star formation by reducing the gas density at the centres of collapsing haloes. The fact that we have confirmed the results in MBH06 (which were mostly inferences obtained by extrapolating from higher redshifts since we were unable to continue those simulations to low enough redshifts) suggests that overall feedback is fairly insensitive to the large-scale environment, overdensity and redshift-dependent halo parameters, and can accurately be modelled in this regime with just the intensity of the impinging UVB.

We note that a value of $J_{21}^{\rm LW} \sim 10^{-3}$–$10^{-2}$ separates feedback regimes dominated by the LWB from those dominated by the transient UVB. As discussed in section 5, there is some uncertainty in these values due to our optically thin treatment. In particular, accounting for LW self-shielding may increase the values of $J_{21}^{\rm LW}$ quoted here.

Additionally, we discover a second episode of eventual positive feedback in haloes which have not yet collapsed when their progenitor regions were exposed to the transient UVB. Gas in such late-forming objects did not have time to set up a steep density profile, which would translate into a strong pressure shock when photoheated. Instead they formed out of material which was of more moderate densities at $z_{\rm UVB,on}$ where the lasting impact of the transient UVB was positive: seeding the gas with an enhanced abundance of molecular hydrogen, which aids in its eventual cooling. However, this feedback regime is very sensitive to the presence of LW radiation, and disappears under fairly modest background intensities of $J_{\rm LW} \gtrsim 10^{-3} \times 10^{-21}\,{\rm erg\,s^{-1}\,cm^{-2}\,Hz^{-1}\,sr^{-1}}$. Nevertheless, when exposed to the same LWB, haloes inside relic H II regions always have a higher H_2 abundance and shorter cooling times than haloes outside relic H II regions, allowing gas to cool faster once it finally begins to collapse on to the halo. Although it is difficult to accurately estimate the build-up of the LWB, it seems likely that such modest values were surpassed well before the bulk of reionization (Haiman et al. 2000). Thus, this persistent eventual positive feedback might only be of academic interest, provided LW self-shielding is not efficient.

We conclude that radiative feedback from a short-lived UVB seems unlikely to have a major impact on the progress of global cosmological reionization, provided that present estimates of the luminosities and lifetimes of Pop III stars are accurate (e.g. Schaerer 2002). Thus, it is likely that the LWB plays the dominant role in regulating feedback in relic H II regions.

ACKNOWLEDGMENTS

We thank the referee for comments which significantly improved the presentation of this paper. Support for this work was provided by NASA through Hubble Fellowship grant HF-01222.01 to AM, awarded by the Space Telescope Science Institute, which is operated by the Association of Universities for Research in Astronomy, Inc., for NASA, under contract NAS 5-26555. GB acknowledges support from NSF grants AST-05-07161, AST-05-47823 and AST-06-06959, as well as computational resources from the National Center for Supercomputing Applications. ZH thanks the Polányi Program of the Hungarian National Office of Technology.

REFERENCES

Abel T., Bryan G. L., Norman M. L., 2002, Sci, 295, 93
Abel T., Wise J. H., Bryan G. L., 2007, ApJ, 659, L87

Ahn K., Shapiro P. R., 2007, MNRAS, 375, 881
Alvarez M. A., Bromm V., Shapiro P. R., 2006, ApJ, 639, 621
Barkana R., Loeb A., 1999, ApJ, 523, 54
Bromm V., Coppi P. S., Larson R. B., 2002, ApJ, 564, 23
Bryan G. L., 1999, Comput. Sci. Eng., 46, 1
Cen R., 2003a, ApJ, 591, L5
Cen R., 2003b, ApJ, 591, 12
Ciardi B., Ferrara A., Abel T., 2000, ApJ, 533, 594
Dijkstra M., Haiman Z., Rees M. J., Weinberg D. H., 2004, ApJ, 601, 666
Dunkley J. et al., 2009, ApJS, 180, 306
Efstathiou G., 1992, MNRAS, 256, 43p
Eisenstein D. J., Hu W., 1999, ApJ, 511, 5
Glover S. C. O., Abel T., 2008, MNRAS, 388, 1627
Gnedin N. Y., 2000, ApJ, 542, 535
Haiman Z., Bryan G. L., 2006, ApJ, 650, 7
Haiman Z., Holder G. P., 2003, ApJ, 595, 1
Haiman Z., Rees M. J., Loeb A., 1996, ApJ, 467, 522
Haiman Z., Rees M. J., Loeb A., 1997, ApJ, 484, 985
Haiman Z., Abel T., Rees M. J., 2000, ApJ, 534, 11
Iliev I. T., Shapiro P. R., Raga A. C., 2005, MNRAS, 361, 405
Johnson J. L., Greif T. H., Bromm V., 2007, ApJ, 665, 85
Kitayama T., Ikeuchi S., 2000, ApJ, 529, 615
Kitayama T., Yoshida N., Susa H., Umemura M., 2004, ApJ, 613, 631
Komatsu E. et al., 2009, ApJS, 180, 330
Kuhlen M., Madau P., 2005, MNRAS, 363, 1069
McGreer I. D., Bryan G. L., 2008, ApJ, 685, 8
Machacek M. E., Bryan G. L., Abel T., 2001, ApJ, 548, 509
Mesinger A., Dijkstra M., 2008, MNRAS, 390, 1071
Mesinger A., Bryan G. L., Haiman Z., 2006, ApJ, 648, 835 (MBH06)
Naoz S., Barkana R., Mesinger A., 2009, MNRAS, in press (arXiv:0906.0349)
Navarro J. F., Frenk C. S., White S. D. M., 1996, ApJ, 462, 563
Norman M. L., Bryan G. L., 1999, in ASSL Vol. 240, Numerical Astrophysics. p. 19
Oh S. P., Haiman Z., 2002, ApJ, 569, 558
Oh S. P., Haiman Z., 2003, MNRAS, 346, 456
O'Shea B. W., Norman M. L., 2008, ApJ, 673, 14
O'Shea B. W., Abel T., Whalen D., Norman M. L., 2005, ApJ, 628, L5
Ricotti M., Gnedin N. Y., Shull J. M., 2001, ApJ, 560, 580
Ricotti M., Gnedin N. Y., Shull J. M., 2002, ApJ, 575, 49
Schaerer D., 2002, A&A, 382, 28
Schaerer D., 2003, A&A, 397, 527
Shapiro P. R., Kang H., 1987, ApJ, 318, 32
Shapiro P. R., Iliev I. T., Raga A. C., 2004, MNRAS, 348, 753
Spergel D. N. et al., 2003, ApJS, 148, 175
Susa H., Umemura M., 2004, ApJ, 600, 1
Susa H., Umemura M., 2006, ApJ, 645, L93
Whalen D., Abel T., Norman M. L., 2004, ApJ, 610, 14
Whalen D., O'Shea B. W., Smidt J., Norman M. L., 2008, ApJ, 679, 925
Wise J. H., Abel T., 2007, ApJ, 671, 1559
Wise J. H., Abel T., 2008a, ApJ, 684, 1
Wise J. H., Abel T., 2008b, ApJ, 685, 40
Wyithe J. S. B., Loeb A., 2003, ApJ, 588, L69
Yoshida N., Oh S. P., Kitayama T., Hernquist L., 2007, ApJ, 663, 687
Yoshida N., Omukai K., Hernquist L., 2008, Sci, 321, 669

This paper has been typeset from a TEX/LATEX file prepared by the author.